Development of a Deep Silicon Phase Fresnel Lens Using Gray-Scale Lithography and Deep Reactive Ion Etching

Brian Morgan, Christopher M. Waits, *Student Member, IEEE*, John Krizmanic, and Reza Ghodssi, *Member, IEEE*

Abstract—We report the first fabrication and development of a deep phase Fresnel lens (PFL) in silicon through the use of gray-scale lithography and deep-reactive ion etching (DRIE). A Gaussian tail approximation is introduced as a method of predicting the height of photoresist gray levels given the relative amount of transmitted light through a gray-scale optical mask. Device mask design is accomplished through command-line scripting in a CAD tool to precisely define the millions of pixels required to generate the appropriate profile in photoresist. Etch selectivity during DRIE pattern transfer is accurately controlled to produce the desired scaling factor between the photoreist and silicon profiles. As a demonstration of this technology, a 1.6-mm diameter PFL is etched 43 μm into silicon with each grating profile designed to focus 8.4 keV photons a distance of 118 m. [1128]

Index Terms—Deep-reactive ion etching (DRIE), gray-scale lithography, phase Fresnel lens (PFL), three-dimensional (3-D) structures.

I. INTRODUCTION

$\mathbf{S}$UFFICIENTLY good angular resolution of a telescope translates into the capability to resolve the fine structure of an astronomical object and to separate multiple objects from each other. However, the angular resolution of X-ray and gamma-ray telescopes have suffered from the difficulty in constructing concentrating optics due to the inherent nature of this high-energy radiation. In fact, the best angular resolution in the 100–1000 keV range offered by current imaging instruments (INTEGRAL, angular resolution of 12 arcminutes [1]) leads to a resolving power of approximately half the angular size of a full moon (31 arcminutes).

Recently, Skinner proposed a Fresnel lens-based system for astronomical observations at hard X-ray and gamma-ray energies [2], [3]. This system would have the highest diffraction-limited angular resolution of any wavelength band,

B. Morgan, C. M. Waits, and R. Ghodssi are with the Department of Electrical and Computer Engineering and the Institute for Systems Research, University of Maryland, College Park, MD 20742 USA (e-mail: bmorgan2@glue.umd.edu; cmwaits@glue.umd.edu; ghodssi@eng.umd.edu).

J. Krizmanic is with the Universities Space Research Association/Laboratory for High Energy Astrophysics, NASA Goddard Space Flight Center, Greenbelt, MD 20771 USA (e-mail: jfk@cosmicra.gsfc.nasa.gov).
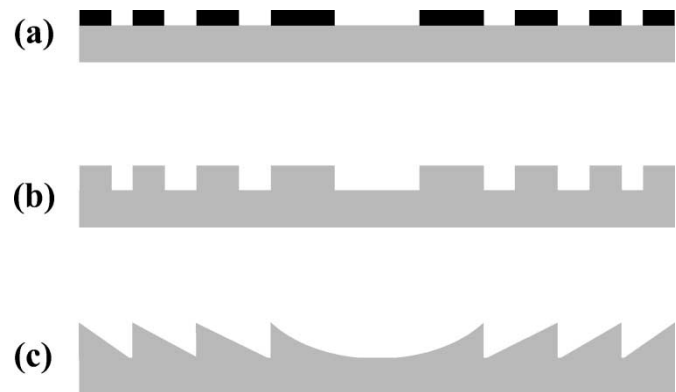
Fig. 1. (a) FZP. (b) PZP or "binary" lens. (c) PFL.

resulting in a greater than 10^8 improvement over current gamma-ray imaging systems. The sensitivity of the proposed system would also be tremendous compared to typical background-limited gamma-ray instruments, resulting in a 10^3 improvement. (Improvements based upon comparison of a 5-m Fresnel lens-based system to that of INTEGRAL [3].) The main drawback will be the inherently long focal length, on the order of 10^6 km, requiring that the lens and detector be located on separate spacecraft and aligned appropriately. (A detailed mission study [4] indicated that given current propulsion technology, a large focal length should not be prohibitive.) The proposed Fresnel lens-based system has the potential to image previously unattainable events such as black hole event horizons, line emission from supernovae, and galactic microquasars.

A Fresnel zone plate (FZP) [Fig. 1(a)] is a small grating that will diffract incident radiation toward its focus. As the off-axis (radial) distance is increased, higher deflection angles are required and thus the width of each diffraction grating becomes smaller. Yet an FZP is limited to an efficiency of only 10.1% because the alternating opaque zones block half of the incident radiation and not all of the energy is transferred to the primary focus, some unfocused energy passes to higher order foci. The Phase Zone Plate (PZP), or "binary" lens [Fig. 1(b)], is an improvement on the FZP design since a phase shift of π is selectively introduced by replacing the opaque zones with slightly thicker regions of the lensing material, raising the theoretical efficiency limit to 40.4%. Ideally, the induced phase change within each zone should be a continuous function of radius, which leads to the cuneiform, or phase Fresnel lens (PFL)

[Fig. 1(c)]. Thus, in a PFL, all of the incident power should be directed into the primary focus, resulting in a theoretical efficiency limit of 100%.

To first demonstrate the superior imaging properties of a PFL, a number of scaled down lenses must be developed for ground testing at lower energies, such as X-rays. Due to the inherently long focal length of PFLs at X-ray energies, a ground test lens of appreciable diameter (>1 mm) must have outer grating widths on the order of tens of micrometers so the focal length will fit inside a testing setup of reasonable dimensions (<0.5 km). Fortunately, silicon is an excellent choice for the lens material because it has low absorption properties at energies between 1 keV (soft X-rays) and 100 keV (soft gamma-rays). Thus by choosing silicon as the lens material, we may take advantage of the plethora of technologies available and under development in the area of micro-fabrication. Gray-scale technology is capable of fabricating three–dimensional (3-D) structures on the necessary scale without alignment—a critical aspect for lens applications where misalignment between gratings will reduce lens performance. Additionally, since our target depths are beyond the normal limits of standard reactive ion etching (RIE) or ion milling, deep reactive ion etching (DRIE) can be used as the method of transferring the photoresist structure into the silicon.

Recently, the use of DRIE to transfer 3-D photoresist structures was briefly demonstrated and patented [5], but its use has been avoided in many applications due to the scalloping effect from standard Bosch processing [6]. However, since the index of refraction of silicon at X-ray energies is close to that of a vacuum, extreme roughness tolerances are not necessary. Furthermore, test lenses should be insensitive to small, localized imperfections introduced during the fabrication process because the image is formed from the integrated effect across the entire device, making local imperfections less significant.

This paper describes the design and fabrication of a PFL to be tested by NASA at the Marshall X-ray Calibration Facility (XRCF) in Huntsville, AL. Tight process control enables a profile prediction method, while careful tuning of etch selectivity produces the desired structure height in silicon.

II. BACKGROUND

A. Silicon Lens Using Gray-Scale Technology

A range of microlens fabrication techniques have been demonstrated over the past decade [7]–[9]. Specifically, binary and stepped PFLs have been fabricated in silicon and other materials by a number of groups [10]–[14]. X-ray Fresnel lenses are probably the most commonly fabricated, yet the dimensions of an astronomical ground test lens in silicon are quite different than those currently used in most X-ray applications [15]–[17]. First, grating widths may be up to 100 times larger than gratings used in other systems. Second, the silicon ground test lens must be much deeper (>20 μm) to achieve the appropriate phase shift through the silicon.

Gray-scale technology easily satisfies these requirements as 3-D structures with various dimensions are routinely created in a single lithography step [18] and silicon etch depths greater than >20 μm are standard in most DRIE applications.

Gray-scale mask design and lithography can be approached in a number of ways, however, all methods rely on the same
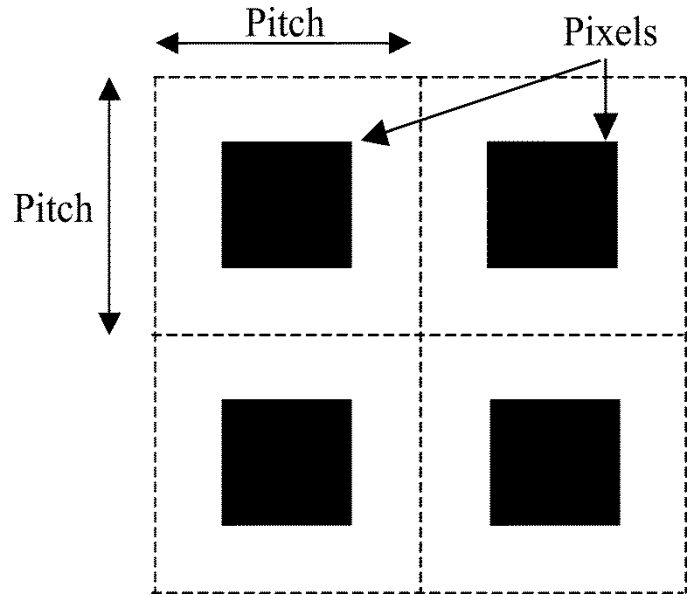

Fig. 2.   Optical mask design scheme using subresolution pixels. By calculating the area of each pixel and the area of the pitch, the percent transmission through the mask is estimated.

general principles [19]–[21]. By modulating the intensity of light through a gray-scale optical mask, a positive photoresist is partially exposed to different depths. After development, a 3-D profile made of "gray levels" will remain in the photoresist corresponding to the intensity pattern generated on the optical mask. The structure can then be etched anisotropically into the silicon.

For this research, a projection lithography method was employed, as outlined by Waits *et al.* [18], which uses a set of subresolution opaque pixels and a fixed center-to-center subresolution spacing, or "pitch" (see Fig. 2.) The intensity seen on the photoresist surface is then proportional to the relative amount of light blocked by the opaque pixel, or equivalently, the percentage of light transmitted through the optical mask. By calculating the area of each pixel (A_{pixel}) and the area of the pitch (A_{pitch}), we can estimate the percent transmission through the mask (Tr) as

$$\text{Tr} = 1 - \frac{A_{\text{pixel}}}{A_{\text{pitch}}}. \qquad (1)$$

The partial transmission through the optical mask coupled with time of exposure, time of development, and photoresist contrast, will determine the final gray level height in photoresist.

B. Lens Design

The thickness (t) of a PFL, as a function of radius (r), is defined as [22]

$$t(r) = t_{2\pi} * \text{MOD}\left[\left(\frac{r}{A}\right)^2, 1\right] \qquad (2)$$

where $t_{2\pi}$ is the thickness of material required to produce a phase shift of 2π, and A is a function of focal length (f) and target photon energy (E), given by

$$A = 49.8 * \sqrt{\frac{f\,(\text{m})}{E\,(\text{keV})}}\ \mu\text{m}. \qquad (3)$$
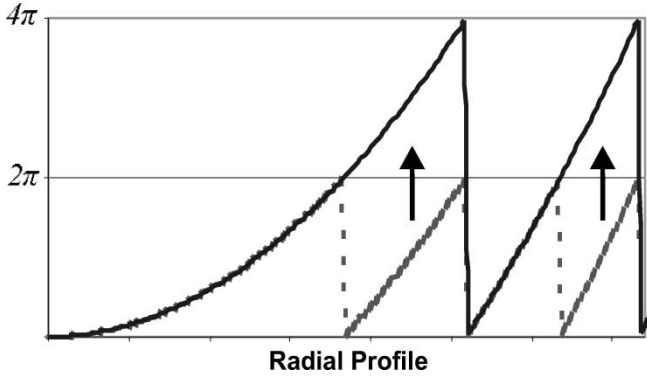
Fig. 3. The 4π phase depth shifts every other grating vertically. This effectively doubles the width of each grating when fabricated in photoresist.
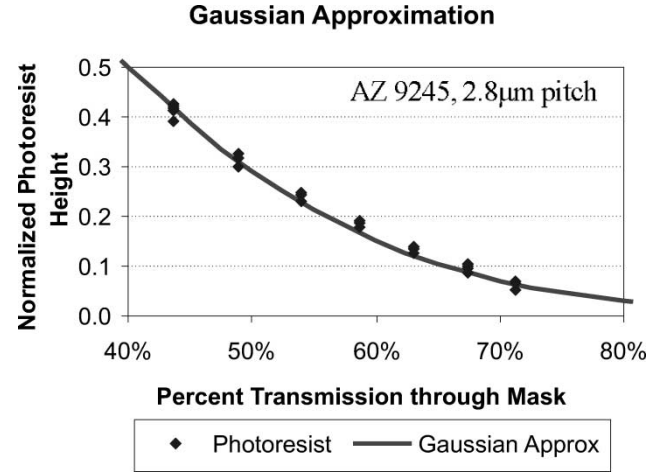

Fig. 4. Gaussian tail approximation relating the normalized height in photoresist to the calculated percentage of light transmitted through the optical mask.

Since limitations are imposed by the mask fabrication system and the chosen method of gray-scale patterning, gray-scale lithography cannot presently guarantee a perfectly contoured lens. Instead a step approximation to the ideal case must be made. As intuition dictates, a larger number of gray levels means a better step approximation to the desired profile, resulting in a lens with higher efficiency. Studies have been done regarding this improvement and a relation derived to predict the efficiency (η) of a multilevel diffractive lens, given the number (N) of steps used [23]–[25]

$$\eta_{\text{Lens}} = \left[\frac{\sin\left(\frac{\pi}{N}\right)}{\left(\frac{\pi}{N}\right)} \right]^2. \tag{4}$$

Therefore, using (4), a binary lens (2 steps) will have a maximum theoretical efficiency of 40.5%. If the number of steps is merely increased to 8, for example, the maximum theoretical efficiency reaches 95.0%. Furthermore, PFLs are not required to produce only a 2π phase shift. Equivalent lenses may be fabricated by increasing the phase depth to 4π, 6π, etc. [26]. If m is the number of 2π phase depths, (2) becomes

$$t(r) = m * t_{2\pi} * MOD\left[\left(\frac{r}{\sqrt{m} * A}\right)^2, 1\right]. \tag{5}$$

The main difference seen with a deeper phase depth is that every other grating is shifted vertically by a 2π phase depth (see Fig. 3). There are two drawbacks of using a deeper phase depth: first, there will be an increase in absorption in the extra material beneath the alternating gratings. Second, since our gray levels are now spread out over 2 phase depths, the number of gray levels must double in order to maintain the same maximum theoretical efficiency. For our PFLs, these drawbacks are minor since silicon was chosen for its low absorption and gray-scale technology has many gray levels available. Additionally, by moving to a deeper phase depth, the horizontal dimensions of each grating in photoresist have effectively been doubled, making them easier to achieve in photoresist on a consistent basis.

III. Experiment

A. Lithography Calibration and Gaussian Approximation

Since gray-scale lithography relies on different light intensities exposing a photoresist to different depths, the photore-sist chosen should preferably be low contrast to maximize the number of achievable gray levels. For this research, Clariant's AZ9245 positive photoresist was chosen for the lithography processing, spun to a nominal thickness between 6 and 7 μm.

A gray-scale calibration mask was designed with a wide range of pixels and pitches to experimentally investigate the main characteristics of our lithography processing and to obtain the best useable range of pixels. Photoresist height measurements taken from the calibration mask were plotted according to their corresponding percent transmission through the optical mask. This data was then fit with a Gaussian curve. By defining two parameters, A_0 and γ, we were able to predict the height in photoresist of future structures according to the transmission through the optical mask

$$H_P = A_0 * \exp\left(-\left(\text{Tr}\right)^2 * \gamma\right) \tag{6}$$

where H_P is the gray level height in photoresist and Tr is the percent transmission through the mask defined in (1). Fig. 4 shows the Gaussian fit for five samples of AZ9245 photoresist for a pitch of 2.8 μm on the optical mask, where $A_0 = 1.28$ and $\gamma = 5.9$.

Depending on the photoresist and developer solution being used, equivalent approximations may also be made in a slightly simpler exponential form

$$H_P = A_0 * \exp\left(-\text{Tr} * \gamma\right). \tag{7}$$

Either approximation method could incorporate small offsets in x or y for improved accuracy.

Equation (6) can be reversed to determine what percent transmission is necessary to produce a desired height

$$\text{Tr} = \sqrt{\frac{-\ln\left(\frac{H_P}{A_0}\right)}{\gamma}}. \tag{8}$$

Using (1), we then obtain an equation that determines the optimum pixel area (A_{pixel}) given the area of the pitch being used (A_{pitch}), the Gaussian parameters $(A_0$ *and* $\gamma)$, and the desired
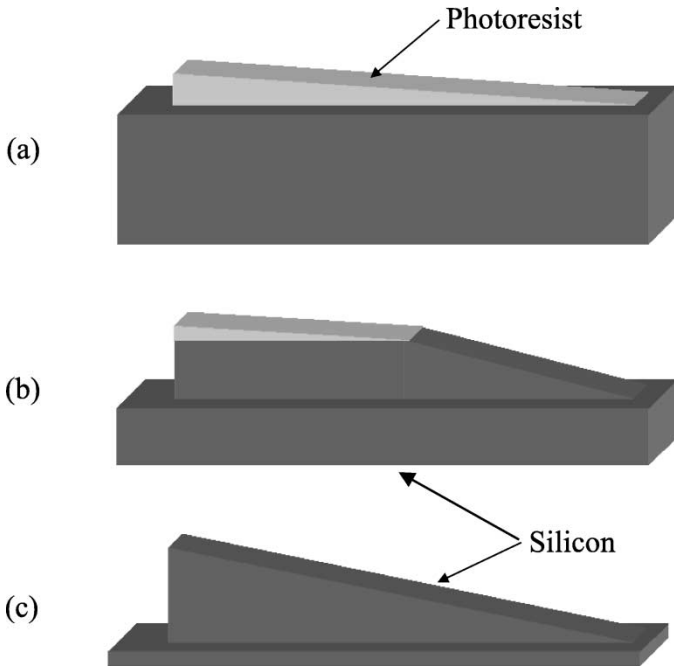
Fig. 5. (a) Initial sloped photoresist structure on silicon. (b) Sloped pattern begins to transfer into the silicon with a selectivity of 4:1. (c) Final structure in silicon retains lateral dimensions while vertical dimensions are amplified four times by the etch selectivity.

height in photoresist (H_P), where H_P is determined by normalizing (5) to peak at the maximum gray level height

$$A_{\mathrm{pixel}} = A_{\mathrm{pitch}} * \left[1 - \sqrt{\frac{-\ln\left(\frac{H_P}{A_0}\right)}{\gamma}} \right]. \qquad (9)$$

This Gaussian approximation method allowed for easy integration into C programming to precisely define the millions of pixels required to produce our complex gray-scale structures. Command-line scripting was then used to import our design into a CAD layout tool.

B. Deep Reactive Ion Etching (DRIE)

A Unaxis, Plasma-Therm 770 ICP etching system with Bosch processing was used for DRIE. Since the vertical dimensions of each structure are entirely dependent upon the selectivity of silicon to photoresist during DRIE (see Fig. 5), precise control of the etch selectivity is paramount to the success of gray-scale technology.

Wedge structures on the calibration mask were etched to investigate the transfer of the gray levels into silicon. Process parameters adjusted while etching the wedges include: etch/passivation times, electrode power, chamber pressure, SF_6 flow, and O_2 flow. Etch recipes were then optimized to give the appropriate selectivity in order to achieve the necessary thickness across each lens.

Once a set etch recipe had been established, (9) was modified to include the desired height in silicon (H_S), total thickness of
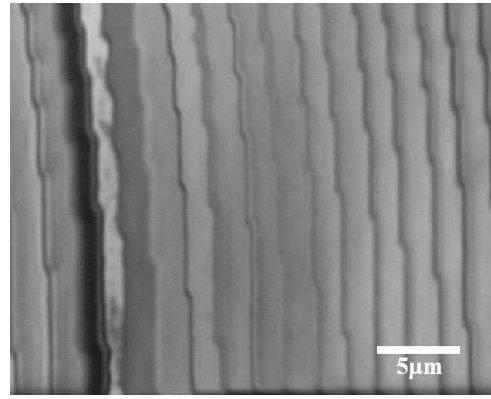

Fig. 6. Digital nature of gratings due to the pixilation method used.

photoresist used (H_0), and the scaling factor (S) introduced by the etch selectivity during DRIE

$$A_{\mathrm{pixel}} = A_{\mathrm{pitch}} * \left[1 - \sqrt{\frac{-\ln\left(\frac{H_S}{S*H_0*A_0}\right)}{\gamma}} \right]. \qquad (10)$$

Equation (10) then makes it possible to relate the desired structure height in silicon directly to the pixel size on the optical mask.

IV. RESULTS AND DISCUSSION

A. Final Device

A 1.64 mm diameter PFL composed of 10 individually profiled gratings and 32 gray levels has been designed and fabricated to demonstrate this technology. Since the lens was designed to be etched to a 4π phase depth in the silicon, 32 gray levels were selected to ensure there would be at least 16 gray levels per phase depth. Thus, using (4), the maximum theoretical efficiency is sufficiently high at 98.7%. The focal length was designed to be 118 m in order to fit reasonably in the test setup at Marshall's XRCF. A pitch of 2.8 μm was used on the optical mask, determined by the resolution of our projection lithography system. After 5 $\times$ optical reduction, we obtained an estimated horizontal resolution of $\sim$0.56 μm on the wafer. The widest grating is 260 μm while the thinnest grating is 40 μm.

B. Lithography Results

Since all pixels were defined in an X-Y layout, there was a digital nature to the profile as each grating curved through its entire 360°. This digital nature of a single grating is shown in Fig. 6, where each thin, jagged strip is a separate gray level with a different height. Although the shift may seem quite dramatic in a single gray level, the overall effect of these shifts is relatively small in comparison to the entire grating width ($>40\,\mu$m). After DRIE transfer, this digital nature is largely washed away by the small amount of isotropic etching during each etch cycle. However, as grating dimensions are reduced, the digital nature will become a larger fraction of the grating width, possibly requiring a smaller pitch to be used on the optical mask for better horizontal resolution.

Metrology measurements were also taken to confirm that our photoresist grating profile was indeed the contour designed
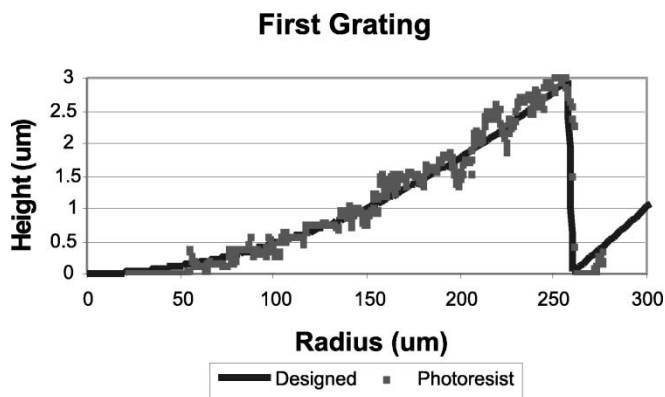
First Grating

Fig. 7. Profile of the first grating of a photoresist PFL compared with the designed case.
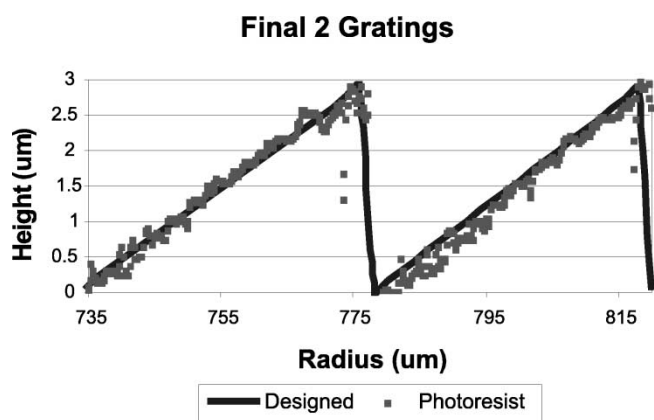
Final 2 Gratings

Fig. 8. Profile of the final two gratings of a photoresist PFL compared with the designed case.

using our Gaussian approximation. Contact profilometry was avoided since it can damage photoresist and is limited by the radius of the tip, often 1–2 μm, which in some cases would be larger than the photoresist gray level we wished to investigate. Therefore, we elected to use an optical profiling system (Veeco, Wyko NT1100) to investigate the success of our profiles. Figs. 7 and 8 show the normalized designed photoresist profile (H_P) and the resulting measurements taken from one of our photoresist samples. We attribute the scattering of data points partially to our gray level step approximation and partially to scattered reflected light from a thin (20 nm) gold coating required by the optical profiler when measuring photoresist. Both figures show excellent agreement between the desired profile and photoresist samples. Similar results have been achieved on a consistent basis.

C. DRIE Results

A multitude of lenses may be produced by etching the same photoresist pattern with a different etch selectivity. The target energy will change as the depth changes, but there is some flexibility as the lens could be used as a 2π or 4π lens depending on the energy being considered. Also, since the lens will focus a range of energies, deviations from the correct depth will result in deviations from the peak performance energy. Concurrently, changes in the focal length may occur as the lens is adapted for

different applications. These points merely emphasize the importance of etch selectivity control to define all vertical dimensions.

The L_alpha line of a tungsten target is strongest at 8.4 keV and was selected for the first demonstration of a PFL using gray-scale technology and DRIE. At 8.4 keV, the 2π phase depth is 21.4 μm in silicon; so for a 4π phase depth, the final structure height of our silicon lens should be 42.8 μm. Using the fact that the lens profile in photoresist was previously measured to be 3 μm tall, we determined that an etch selectivity of silicon to photoresist $<15:1$ was necessary to obtain the designed structure height. This target selectivity is, significantly lower than traditional DRIE selectivities ($\sim$80:1).

To accomplish such a unique etch, an extra step containing only O_2 and Ar was added to the standard Bosch cycle after the usual passivation and etch steps. During this step, only the photoresist is briefly etched while the silicon profile remains essentially unchanged. In this way, a small slice of the photoresist is removed after each cycle and the pattern is transferred with a significantly lower selectivity than would be produced by only the usual etch steps. Presumably some vertical resolution is sacrificed by introducing this extra step during each cycle to lower the selectivity, as some gray levels may be lost. However, $\sim$100 cycles were necessary to fully transfer this 3 μm photoresist pattern, meaning only photoresist features <0.03 μm will be consumed during the step containing just O_2 and Ar. Assuming a selectivity of 15:1, our vertical resolution in silicon was estimated to be $\sim$0.45 μm. The resultant silicon PFL is shown in Fig. 9.

Optical profilometry was used to verify our etch depth. Fig. 10 shows a contour map of the innermost grating taken with the WYKO system used earlier. (A gold coating not required when measuring silicon.) We were able to define a circle on this map and measure the height of our grating along the circumference of this circle. The circumference measured is illustrated on Fig. 10. The top of the lens was measured to be 42.5 μm (standard deviation $= 0.70$ μm), less than 1% error from our design. A lens with an average height of 42.5 μm will exhibit peak efficiency at 8.33 keV rather than the designed 8.4 keV. The individual gray level roughness (RMS) was measured to be 0.4 μm. Nonuniformity and height errors can possibly be attributed to factors such as data leveling in the analysis software, or photoresist and etch nonuniformity which have previously been investigated [27].

D. Discussion

Gray-scale lithography suffers from the fact that processing is heavily dependent on many factors. Some factors can be controlled, such as choosing a photoresist with the appropriate contrast or developer concentration. Yet, a large number of factors can only be controlled in a limited sense, such as projection lithography equipment parameters like resolution, or optical mask fabrication limitations. Process tolerances must also be extremely tight in order to ensure reproducibility. All of these factors make transferring a gray-scale process from one lab to another extremely difficult, as each lab exhibits small changes in environment and equipment, causing the gray-scale operating range to change dramatically.
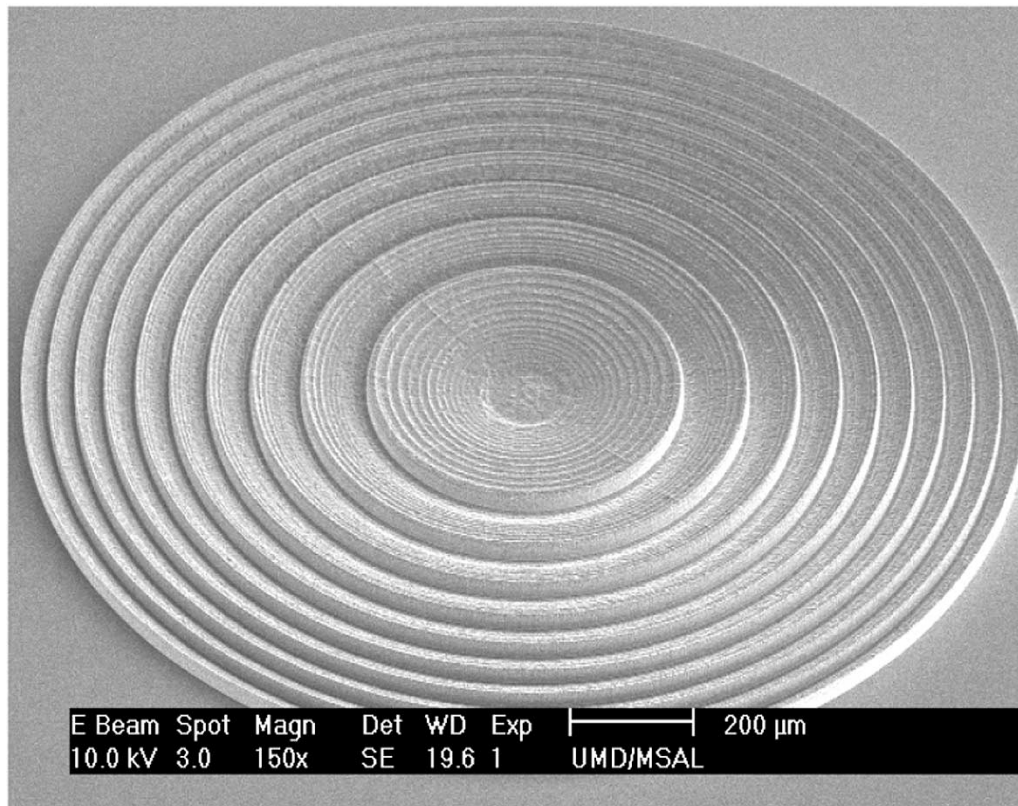
Fig. 9. PFL consisting of 10 profiled gratings for X-ray diffraction, where each grating has a uniquely defined profile. The lens diameter is 1.6 mm and has been etched 42.5 μm into the silicon.
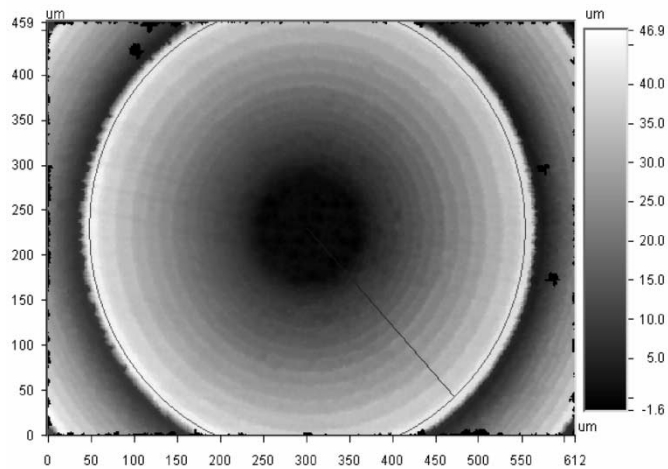

Fig. 10. Contour map of first grating. Overlaid circle marks the area being measured to obtain the vertical height of the lens.

The Gaussian approximation method developed and demonstrated above enables any user of gray-scale technology to experimentally investigate the properties of their individual lithography process. By using a calibration mask, a fixed lithography process may be established that fits the user's other requirements, such as photoresist contrast or sidewall profile. By then employing the Gaussian approximation, a useable range of pixel sizes can be identified and easily integrated into device design. The Gaussian approximation is thereby a method of consolidating the many factors in a lithography process into a simple model, making the understanding of each individual factor unnecessary. Processing changes may be quickly accounted for by re-calibrating the approximation after, for example, changing photoresists. As shown earlier in Figs. 7 and 8, the Gaussian approximation performed quite well in our process conditions.

Although relatively unimportant in PFL design, gray-scale lithography will exhibit some drawbacks when applied to other MEMS areas. Since the method of design is a pixelated one, there is a loss of resolution, which may or may not be acceptable in certain applications. Also, as structure sizes increase, optical mask layout files may approach 1 gigabyte in size, making files cumbersome to work with and optical masks expensive to fabricate. Photoresist sidewall profile and linewidth control may also be sacrificed when working in a gray-scale regime where the exposed photoresist is barely removed.

While DRIE transfer of gray-scale and planar structures can be accomplished simultaneously, there is a tradeoff between etch characteristics that will have varying importance depending on the application. Normally etch characteristics are tailored to reach acceptable values by changing parameters such as chamber pressure. However, in most applications the selectivity must fall only within a small range, so resulting changes in selectivity are often ignored. When etching gray-scale structures, etch selectivity determines the vertical dimensions of each gray-scale structure, and therefore must take precedence over all other etch characteristics, such as sidewall profile or etch rate.

For applications such as the fabrication of the PFL presented in this paper, ultra low selectivity may be required, which means

TABLE I
MODULATING THE LENGTH OF THE O_2 STEP AND THE
RESULTING ETCH SELECTIVITY

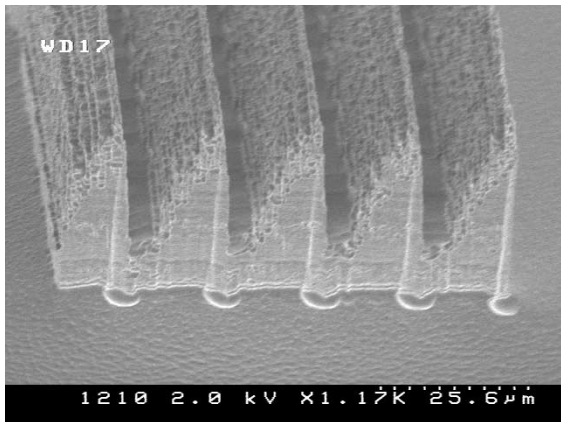| Etch	Length of O_2 Step (sec)	Etch Selectivity
1	0	70.4
2	2	37.2
3	4	25.6
4	6	13.7

Fig. 11. Narrow gratings (<20 μm) on test structures do not etch as deeply as open areas and wide gratings.

drastic process changes and almost certainly changes in sidewall profiles. One of the major advantages of using an extra O_2 step is that changing the duration of that step can modulate the selectivity (see Table I). Since the O_2 step should only affect the photoresist and not the silicon, sidewall profiles should remain unchanged. In this way the usual Bosch steps may be adjusted to give beneficial etch characteristics like vertical sidewalls and minimum roughness, while the O_2 step can be adjusted to compensate for any resulting changes in etch selectivity.

A problem that has long plagued DRIE in many applications is aspect ratio dependent etching (ARDE), where trenches of different widths etch to different depths [28]. This can be seen in Fig. 11 where the silicon between narrow gray-scale gratings (<20 μm) is not etched to the same depth as the open area and wider gratings. Gray-scale technology can provide a possible solution by incorporating a small offset when designing a structure. Higher gray levels may be used at the bottom of the wide gratings to locally increase the photoresist thickness. Accordingly, the silicon between the narrow gratings will begin etching while the extra photoresist height is slowly removed between the wider ridges, essentially giving the narrow gratings a head start. By carefully monitoring etch progress, the point at which the wide gratings "catch" the narrow gratings can be identified and the etch depth is no longer aspect ratio dependent. This concept will be investigated as PFLs with larger diameters, and more narrow gratings, are developed.

V. CONCLUSION

We have presented a method for precisely designing and fabricating arbitrary 3-D profiles in silicon. A simple Gaussian ap-

proximation was shown to provide accurate photoresist profile prediction in a format that can be easily integrated into command-line scripting in a CAD tool. A 1.6-mm diameter PFL was designed using this approximation method while balancing process tolerances and design requirements. A DRIE etch selectivity of 15:1 was achieved through the introduction of an additional step, containing only O_2 and Ar, to the traditional Bosch cycle. This low etch selectivity enabled the full transfer of the photoresist PFL into silicon to achieve the appropriate phase shift at each point on the lens. With a maximum theoretical efficiency of 98.7%, even with fabrication errors, such a stepped PFL should exhibit a great increase in efficiency over traditional binary Fresnel lenses (40.4%).

Ground testing will be coordinated at NASA Marshall XRCF for all fabricated silicon PFLs. Each lens will be placed in a quasiplanar X-ray beam line to image spot size and interference patterns on a CCD camera, allowing performance parameters, such as angular resolution, to be extracted.

While this paper has demonstrated gray-scale technology using DRIE as a viable option for the fabrication of PFLs in silicon, the methodology and design considerations presented here can be applied to almost any other sloped silicon structures containing arbitrary angles. Further characterization and development of this technology will enable more precise profiles to be achieved for all applications, while working toward highly efficient PFLs for ground testing by NASA.

REFERENCES

[1] (2003, July 24). [Online]. Available: http://sci.esa.int/integral/ visited
[2] G. Skinner, "Diffractive/refractive optics for high energy astronomy I. Gamma-ray phase Fresnel lenses," *Astronomy and Astrophys.*, vol. 375, pp. 691–700, 2001.
[3] G. Skinner, P. von Ballmoos, H. Halloin, N. Gehrels, and J. Krizmanic, "Diffraction-limited gamma-ray imaging with Fresnel lenses," in *Proc. SPIE v.4851, X-Ray and Gamma-Ray Telescopes and Instruments for Astronomy*, J. E. Truemper and H. D. Tananbaum, Eds., 2002.
[4] NASA GSFC Integrated Mission Design Center(IMDC) Study, 2002.
[5] M. R. Whitley, R. L. Clark, J. R. Shaw, D. R. Brown, P. S. Erbach, and G. T. Dorek, "Int. Patent," WO 02/31 600 A1, 2002.
[6] R. B. GmbH, "U.S. Patent," 5 501 893, 1996.
[7] J. Shimada, O. Ohguchi, and R. Sawada, "Microlens fabricated by the planar process," *J. Lightwave Technol.*, vol. 9, pp. 571–576, May 1991.
[8] E.-H. Park, M.-J. Kim, and Y.-S. Kwon, "Microlens for efficient coupling between LED and optical fiber," *IEEE Photon. Technol. Lett.*, vol. 11, pp. 439–441, Apr. 1999.
[9] C. David, B. Nohammer, and E. Ziegler, "Wavelength tunable diffractive transmission lenses for hard x-rays," *Appl. Phys. Lett.*, vol. 79, no. 8, pp. 1088–90, Aug. 2001.
[10] L. Y. Lin, S. S. Lee, K. S. J. Pister, and M. C. Wu, "Micro-machined three-dimensional micro-optics for integrated free-space optical system," *IEEE Photon. Technol. Lett.*, vol. 6, pp. 1445–1447, 1994.
[11] M. J. Zwanenburg *et al.*, *Phys. Rev. Lett.*, vol. 85, p. 5154, 2000.
[12] Y. Li *et al.*, "Characterizing the hard x-ray diffraction properties of a GaAs linear Bragg-Fresnel lens," *Appl. Phys. Lett.*, vol. 77, no. 3, pp. 313–315, July 2000.
[13] E. Di Fabrizio and M. Gentili, "X-ray multilevel zone plate fabrication by means of electron-beam lithography: Toward high-efficiency performances," *J. Vac. Sci. Technol. B*, vol. 17, no. 6, pp. 3439–3443, Nov./Dec. 1999.

[14] E. DiFabrizio, F. Romanato, M. Gentili, R. Gabrini, R. Kaulich, J. Susini, and R. Barrett, "High efficiency multilevel zone plates for keV X-rays," *Nature*, vol. 401, October 1999.

[15] S. Spector, C. J. Jacobsen, and D. M. Tennant, "Process optimization for production of sub-20 nm soft x-ray zone plates," *J. Vac. Sci. Technol. B*, vol. 15, no. 6, pp. 2872–2876, Nov./Dec. 1997.

[16] Z. Chen *et al.*, "Design and fabrication of Fresnel zone plates with large numbers of zones," *J. Vac. Sci. Technol. B*, vol. 15, no. 6, pp. 2522–2527, Nov./Dec. 1997.

[17] C. David and A. Souvorov, "High-efficiency Bragg-Fresnel lenses with 100 nm outermost zone width," *Rev. Scientif. Instrum.*, vol. 70, no. 11, pp. 4168–4173, Nov. 1999.

[18] C. M. Waits, A. Modafe, and R. Ghodssi, "Investigation of gray scale technology for large area 3D silicon MEMS structures," *J. Micromech. Microeng.*, vol. 13, pp. 170–177, 2003.

[19] Canyon Materials Inc., "U.S. Patent," 5 285 517, 1994.

[20] W. Daschner, R. Stein, P. Long, C. Wu, and S. H. Lee, "1996 one-step lithography for mass production of multilevel diffractive optical elements using high energy beam sensitive (HEBS) gray-level mask," in *Proc. SPIE: Diffractive and Holographic Optics Technology III*, vol. 2689, pp. 153–155.

[21] Gal, "U.S. Patent," 5 310 623, 1994.

[22] E. Hecht and A. Zajac, *OPTICS*. Reading, MA: Addison-Wesley, 1974, p. 375.

[23] B. Hadimioglu, E. G. Rawson, R. Lujan, M. Lim, J. C. Zesch, B. T. Khuri-Yakub, and C. F. Quate, "High-Efficiency Fresnel acoustic lenses," in *1993 Ultrasonics Symp.*, pp. 579–582.

[24] J. R. Leger, M. L. Scott, P. Bundman, and M. P. Griswold, "Astigmatic wavefront correction of gain-guided laser diode array using anamorphic diffractive microlenses," in *Proc. SPIE*, vol. 884, 1988, p. 82.

[25] B. H. Kleemann and R. Guther, "Zonal diffraction efficiencies and imaging of micro-Fresnel lenses," *J. Modern Opt.*, vol. 45, no. 7, pp. 1405–1420, 1998.

[26] M. Kuittinen, H. P. Herzig, and P. Ehbets, "Improvements in diffraction efficiency of gratings and microlenses with continuous relief structures," *Opt. Commun.*, vol. 120, pp. 230–234, 1995.

[27] C. M. Waits, B. Morgan, M. Kastantin, and R. Ghodssi, "Microfabrication of 3-D silicon structures using gray-scale lithography and deep reactive ion etching," Sensors and Actuators A: Physical, submitted for publication.

[28] A. Ayon, R. Braff, C. Lin, and H. Sawin, "Characterization of a time multiplexed inductively coupled plasma etcher," *J. Electrochem. Soc.*, vol. 146, no. 1, pp. 339–49, Jan. 1999.

Brian Morgan received the B.S. degree in physics from Georgetown University, Washington, DC, in 2002.

He is currently working toward the Masters degree in electrical engineering at the University of Maryland—College Park, supported under a fellowship awarded by the Army Research Laboratory. His main research interests are in the areas of electrostatic MEMS devices and 3-D fabrication technologies.

Mr. Morgan is a member of the Sigma Xi Scientific Research Society.

Christopher M. Waits (S'01) received the B.S. degree in physics from Salisbury State University, Salisbury, MD, in 2000 and the M.S. degree in electrical engineering from the University of Maryland, College Park, in 2003.

He is currently working toward the Ph.D. degree in electrical engineering at the University of Maryland. His main research interests are in the areas of deep silicon micromachining, power MEMS, and development of 3-D technology.

John Krizmanic received the B.A. degree in physics and mathematics from Northwestern University in 1983, the M.A. degree in physics and the Ph.D. degree, both from the Johns Hopkins University, Baltimore, MD, in 1986 and 1989, respectively.

He is currently with the Universities Space Research Association and is a member of the High Energy Cosmic Ray Group in the Laboratory for High Energy Astrophysics of NASA Goddard Space Flight Center, Greenbelt, MD. Besides diffractive Fresnel lens development, his research interests also include developing semiconductor detectors for astrophysical measurements and developing and performing astroparticle physics experiments with an emphasis on high-energy cosmic ray measurements.

Reza Ghodssi (M'02) was born in Tehran, Iran, in 1966. He received the B.S., M.S., and Ph.D. degrees in electrical engineering from the University of Wisconsin at Madison, in 1990, 1992, and 1996, respectively. His Ph.D. thesis was focused on development of a high aspect ratio microfabrication process for an electrostatic-driven MEMS device using X-ray lithography and LIGA technology.

He was a Postdoctoral Associate and a Research Scientist with the Microsystems Technology Laboratories and with the Gas Turbine Laboratory at the Massachusetts Institute of Technology (MIT), Cambridge, from 1997 until 1999. During his tenure at MIT, he developed the building block MEMS fabrication technologies for a microturbine generator device and also served as an Assistant Director on that project. In January 2000, he joined the Department of Electrical and Computer Engineering and the Institute for Systems Research at the University of Maryland (UMD) at College Park as an Assistant Professor. His research interests are in design and development of microfabrication technologies and their applications to microsensors, microactuators, and integrative microsystems.

Dr. Ghodssi was awarded the 2001 UMD George Corcoran Award, 2002 National Science Foundation CAREER Award, and the 2003 UMD Outstanding Systems Engineering Faculty Award. He has served as a program co-chairman for the 2001 International Semiconductor Device Research Symposium (ISDRS) and as a chairman of the MEMS Technical Group at the 2002 and 2003 American Vacuum Society (AVS) International Symposiums. He is a cofounder of the MEMS Alliance Group in the greater Washington area and a member of the AVS and MRS societies.